

Published in final edited form as:

*Hepatology*. 2013 February ; 57(2): 786–796. doi:10.1002/hep.26056.

## Reduced Hepatic Stellate Cell Expression of KLF6 Tumor Suppressor Isoforms Amplifies Fibrosis During Acute and Chronic Rodent Liver Injury

Zahra Ghiassi-Nejad<sup>1</sup>, Virginia Hernandez-Gea<sup>1</sup>, Christopher Woodrell<sup>1</sup>, Ursula E. Lang<sup>1</sup>, Katja Dunic<sup>2</sup>, Allison Kwong<sup>1</sup>, and Scott L. Friedman<sup>1</sup>

<sup>1</sup>Division of Liver Diseases, Mount Sinai School of Medicine, New York, NY Department of Gastroenterology and Hepatology

<sup>2</sup>Division of Clinical Genetics, Clinical Hospital Centre “Sisters of Mercy”, Zagreb Croatia, Department of Pediatrics

### Abstract

Kruppel like factor 6 (KLF6), a zinc finger transcription factor and tumor suppressor, is induced as an immediate-early gene during hepatic stellate cell (HSC) activation. The paradoxical induction of a tumor suppressor in HSCs during proliferation led us to explore the biology of wild type KLF6 (KLF6<sub>WT</sub>) and its antagonistic, alternatively spliced isoform KLF6<sub>SV1</sub> in cultured HSCs and animal models.

**Methods**—The animal models generated include a global heterozygous KLF6 mouse (*Klf6*<sup>+/-</sup>), and transgenic mice expressing either *hKLF6*<sub>WT</sub> or *hKLF6*<sub>SV1</sub> under the control of the *Collagen α2 (I)* promoter to drive HSC-specific gene expression following injury.

**Results**—The rat *Klf6* transcript has multiple splice forms that are homologous to those of the human *KLF6* gene. Following a transient increase, all rat *Klf6* isoforms decreased in response to acute CCl<sub>4</sub> liver injury, and culture-induced activation. After acute CCl<sub>4</sub>, *Klf6*<sup>+/-</sup> mice developed significantly increased fibrosis and enhanced fibrogenic mRNA and protein expression. In contrast, HSC-specific transgenic mice over-expressing *KLF6*<sub>WT</sub> or *KLF6*<sub>SV1</sub> developed significantly diminished fibrosis with reduced expression of fibrogenic genes. Chromatin IP, and qRT-PCR in mouse HSCs over-expressing *KLF6*<sub>WT</sub> demonstrated KLF6<sub>WT</sub> binding to GC boxes in promoters of *Colα1 (I)*, *Colα2 (I)*, and *β-Pdgfr* with reduced gene expression, consistent with transcriptional repression by KLF6. Stellate cells over-expressing either *KLF6*<sub>WT</sub> or *KLF6*<sub>SV1</sub> were more susceptible to apoptotic stress based on PARP cleavage.

**Conclusion**—KLF6 reduces fibrogenic activity of HSCs via two distinct mechanisms, direct transcriptional repression of target fibrogenic genes and increased apoptosis of activated HSCs. These results suggest that following its initial induction, sustained downregulation of KLF6 in liver injury may allow de-repression of fibrogenic genes and decreased stellate cell clearance by inhibiting apoptosis.

### Introduction

Our previous efforts to understand the molecular basis of stellate cell activation utilized subtraction hybridization to clone a novel zinc finger transcription factor, *Klf6* (previously called “Zf9”), which is induced as an immediate-early gene in hepatic stellate cells during

liver injury in vivo (1). Subsequent studies have broadened KLF6's roles in injury to include growth responses of vascular endothelial cells and hepatocytes, among others (2, 3). KLF6 is a member of a large family of zinc finger transcription factors that have a conserved C-terminal C<sub>2</sub>H<sub>2</sub> DNA binding domain recognizing "GC box" motifs in responsive promoters. Studies originally performed in liver ultimately led to the identification of KLF6 as a growth-inhibitory tumor suppressor gene that is inactivated in several human cancers (4, 5).

The discovery that *Klf6*, a growth suppressive gene, is rapidly induced when stellate cells undergo a proliferative burst, presented a paradox that the current study has sought to reconcile. In addition to full length KLF6, human *KLF6* has several shorter antagonistic splice isoforms, *KLF6<sub>SV1-3</sub>*; among these, *KLF6<sub>SV1</sub>* is the best studied (6, 7). Based on these information we hypothesized that the cloning of *Klf6* in rat stellate cells (1) actually represented a growth-promoting splice isoform that contributes to stellate cell activation, yet rodent splice isoforms were not described.

In our studies exploring the role of KLF6 during stellate cell activation we employed *Klf6*<sup>+/-</sup> mice, lacking one allele of *Klf6* in all cells; these mice are viable, fertile and phenotypically normal whereas *Klf6* null mice are embryonic lethal (8). We used these animals, in addition to novel stellate cell-specific transgenic mice to explore the role of KLF6 in hepatic stellate cell activation and fibrogenic gene induction.

## Methods

### Semi-quantitative PCR and cloning of rat *Klf6* splice variants

PCR was performed using primers to rat *Klf6* mRNA untranslated regions- 5' UTR: AACTTTCACCTGCGCTCCCG, 3'UTR: TGGCTGGTACAGGTATCCCTC with rat primary stellate cell complementary DNA (cDNA) as a template. The products of the reaction were separated using gel electrophoresis. Bands were excised and extracted using the QIAquick® Gel Extraction Kit (Qiagen, Chatsworth, CA) according to the manufacturer's protocol. The DNA fragments were then cloned into the pCR®8/GW/TOPO® TA vector (Invitrogen, Carlsbad, CA) for sequencing and subsequently into the pcDNA3.1/V5-His® TOPO® TA Expression Kit (Invitrogen, Carlsbad, CA) according to the manufacturer's protocol.

### Animal Studies

All animals received humane care according to the criteria outlined in the "Guide for the Care and Use of Laboratory Animals" prepared by the National Academy of Sciences and published by the National Institutes of Health (NIH publication 86-23 revised 1985).

### Murine and rat stellate cell isolation

Mice were injected intra-peritoneally with CCl<sub>4</sub> (5ul/g mouse of 10% CCl<sub>4</sub> in corn oil) (Sigma) three times (alternating days), and mouse stellate cells were isolated 2 days after the last dose of CCl<sub>4</sub>. mHSCs were isolated from C57/B16 wild type, *Klf6<sup>FF</sup>*, *Cola2(I)-KLF6<sub>WT</sub>* and *Cola2(I)-KLF6<sub>SV1</sub>* mice by enzymatic digestion and Percoll density gradient centrifugation, (9) with modifications. For the transgenic mouse HSC studies, stellate cells were isolated and mRNA was harvested without culturing the cells. For the in vitro KLF6 deletion studies, *Klf6<sup>FF</sup>* HSCs were cultured for 10 days and then infected with either Ad-lacZ or Ad-Cre at an MOI of 10. Viral transduction efficiency was 85% as assessed using Ad-EGFP and fluorescence microscopy. Protein lysates were collected for Western blot.

### Rat *Klf6* isoform quantitation

For liver injury experiments, Sprague-Dawley rats were injected with CCl<sub>4</sub> (2μl/g of a 50% CCl<sub>4</sub> solution in corn oil) or corn oil, followed by isolation of HSCs (see below) at 24 h or 48 h after injection (n=3 for each condition). Messenger RNA was isolated and quantitative RT-PCR (see next section) was performed using isoform-specific primers to identify any rat *Klf6* isoforms (see Table 1 for list of primers). For culture activation experiments, HSCs were isolated from untreated rats and activated by growth in primary culture on non-coated plastic dishes for up to 1 week. Messenger RNA was harvested from the cells at days 0, 2, 4, & 7, in three separate cell isolates.

### Reverse-Transcription and Real-Time Quantitative PCR

RNA was extracted from cells/liver tissue and reverse-transcribed into cDNA using an RNeasy® kit (Qiagen, Valencia, CA) and using Sprint™ RT Complete-Double PrePrimed tubes (Clontech, Mountain View, CA) respectively, and analyzed by quantitative PCR using SYBR green qPCR Master Mix (Roche) on the lightCycler®480 System (Roche). Data are represented as the relative expression of fibrogenic genes after normalizing to GAPDH. Please refer to Table 1 for a complete list of primers.

### Western blot

Western blots of cell extracts were prepared by centrifuging the cells with lysis buffer complemented with protease inhibitor (Complete Lysis-M kit, Roche Diagnostics, Indianapolis, IN) Protein concentration was determined with a Bio-Rad DC kit (Bio-Rad). Antibodies used were as follows: Rabbit anti-Collagen I (1:1000)(Rockland), Rabbit anti-β-PDGFR (1:500)(Santa Cruz), Mouse anti-ASMA (1:500)(Milipore).

### Rat KLF6 degradation analysis

293FT cells were plated in six-well plates and serum starved for four hours prior to transfection. Cells were transiently transfected using the Lipofectamine™ 2000 Reagent (Invitrogen, Chatsworth CA) according to the manufacturer's protocol with pcDNA3.1/rKlf6<sub>top</sub>-V5, pcDNA3.1/rKlf6<sub>mid</sub>-V5, pcDNA3.1/rKlf6<sub>bot</sub>-V5, or pcDNA3.1/V5. 24 hours later cells were either treated with proteasomal inhibitor MG132 (Sigma) at a final concentration of 10μM or an equal volume of DMSO. Protein was harvested 5 hours after addition of MG132.

### Rat KLF6 cellular localization

293FT cells were plated in six-well plates and serum-starved for four hours prior to transfection. Cells were transiently transfected using the Lipofectamine™ 2000 Reagent (Invitrogen, Chatsworth CA) according to the manufacturer's protocol with pcDNA3.1/rKlf6<sub>top</sub>-V5, pcDNA3.1/rKlf6<sub>mid</sub>-V5, pcDNA3.1/rKlf6<sub>bot</sub>-V5, or pcDNA3.1/V5. Cells were fixed with ice-cold methanol, and stained first with monoclonal mouse anti-V5 antibody (1:50)(Abcam), followed by FITC-conjugated goat anti-mouse antibody (1:250) (Invitrogen). Cells were mounted using Vectashield containing DAPI (Invitrogen).

### Generation of HSC-specific *KLF6* transgenic mice

*Colα2(I)-KLF6<sub>WT</sub>* and *Colα2(I)-KLF6<sub>SVI</sub>* constructs were generated by cloning *KLF6<sub>WT</sub>* and *KLF6<sub>SVI</sub>* downstream of the *Colα2(I)* enhancer promoter. These constructs were then used to generate transgenic mice on a C57/B16 background. (Mouse Genetics Shared Resource Facility at Mt. Sinai) The same transgene specific primers were used to identify both *KLF6<sub>WT</sub>* and *KLF6<sub>SVI</sub>* transgene positive founder mice. Geno Fwd: GGAACGGTCCACGATTGCCAAGTCT, Geno Rev:

TAACGTTCCAGCTCTAGGCAGGTCTG. Transgenic lines were selected based on good transgene induction following a single dose of CCl<sub>4</sub>.

### Chronic CCl<sub>4</sub> injury

For chronic CCl<sub>4</sub> experiments, mice were injected intra-peritoneally twice per week for 8 weeks with a dose of (5ul/g mouse of 10% CCl<sub>4</sub> in corn oil) Mice were sacrificed 48h after the last dose of CCl<sub>4</sub>, and liver tissue was collected for mRNA/protein analysis, H&E staining, Sirius Red Staining, and ASMA immunohistochemistry. For the *Klf6*<sup>+/-</sup> mice (n=7 per group), and for the HSC specific transgenic animals (n=6 per group).

### Quantitative fibrosis morphometry in liver sections

Formalin fixed, paraffin embedded liver tissue was stained with Sirius Red. For each animal, 40 images were taken at low magnification (10× objective lens), and were subsequently used for quantifying percentage of fibrotic tissue using BioQuant Software.

### Chromatin immunoprecipitation assays (ChIP)

Chromatin immunoprecipitation assays (ChIP) were performed using a commercial kit according to the manufacturer's instructions (Active Motif-ChIP-IT™ Express). Proteins cross-linked to DNA were immunoprecipitated with 10 μg of anti-KLF6 antibody (0.2 μg/μl) (R-173) (Santa Cruz Biotechnology), 10 μg anti-histone H3 rabbit antiserum (0.2 μg/μl) (07-690) (Upstate Biotechnology, Inc), 10 μg anti-KLF6<sub>SV1</sub> antibody (0.5 μg/μl) (Invitrogen) or 10 μg control IgG (0.4 μg/μl) (sc-2027) (Santa Cruz Biotechnology) and protein-G-magnetic beads. Genomic sequence primers encompassing “GC-boxes” in promoter regions (within 2 kbp) upstream of transcriptional start site were used to amplify immunoprecipitated DNA. *Cola1(I) Fwd*: 5'-CCCTTCCTTCCCTCCTCC-3', *Cola1(I) Rev*: 5'- TGGCCTGGGCCCTTTTAT-3'; *Cola2(I) Fwd*: 5'-CCAGTCCCTCAACACCTG-3', *Cola2(I) Rev*: 5'-AGTGCTGGGAGGAGACTGC-3'; β-*PDGFR Fwd*: 5'-GCGAAAGTGGAAGAGAACCAG-3', β-*PDGFR Rev*: 5'-GGACTAAGTTGTCTGGAACCAC-3'.

### PARP cleavage studies

We employed human HSC line (LX2) stably transfected with Adenovirus containing *pBabe*, *pBabe-KLF6<sub>WT</sub>*, or *pBabe-KLF6<sub>SV1</sub>*. Briefly LX2 cells were infected with adenovirus containing the above sequences and cell selection was performed using puromycin at a concentration of 0.45 μg/ml. Stable colonies were selected at one week, amplified and used in further experiments.

## Results

### Rat *Klf6* is alternatively spliced, with all splice isoforms decreased during stellate cell activation

*Klf6* was first cloned from primary rat stellate cells (1) using subtractive hybridization (10), which yielded a cDNA fragment that was used to screen a full-length, sized cDNA library from stellate cells; this approach led to the isolation of the *Klf6* full length rat cDNA. Using this cloning strategy, we were not able to recognize that the rat *KLF6* transcript might be alternatively spliced. Subsequently, three alternative splice isoforms of human *KLF6* (*hKLF6*) were discovered (*KLF6<sub>SV1-3</sub>*) in the context of carcinogenesis (11). Among these, *KLF6<sub>SV1</sub>*, is the best studied, and has been further identified as a growth promoting isoform that antagonizes the function of full length *KLF6* (“*KLF6<sub>WT</sub>*”) (6, 7, 12). Based on this finding, we then surmised that *KLF6* might also be alternatively spliced during hepatic

stellate cell activation in response to tissue injury, leading to increased generation of an antagonistic splice form that promotes stellate cell activation.

To test this hypothesis, we explored whether *Klf6* was alternatively spliced in rat stellate cells by using RT-PCR based on flanking primer sequences in the rat 5' and 3' KLF6 untranslated regions (UTRs). Using cDNA primary rat stellate cells from untreated animals we consistently detected 3 distinct bands, which were cloned, sequenced, and aligned against the rat genome. This approach yielded 3 novel *rKlf6* splice forms. The *rKlf6* splice forms were labeled 'Top', 'Middle', and 'Bottom' based on their size, shown in Fig. 1A.

Even though the splicing pattern for *rKlf6* is different from *hKLF6*, there are several key similarities. The *rKlf6<sub>top</sub>* (283 aa) corresponds to *hKLF6<sub>WT</sub>*, with a homology of 93% at the amino acid level. A 243 bp stretch of nucleotides of exon 2 (bps 201–443) is spliced out in *rKlf6<sub>mid</sub>* (72aa) and this splicing pattern leads to a frame-shift with a premature stop codon (depicted by \* in Fig. 1A). For *rKlf6<sub>bot</sub>* (55aa), there is a complete skipping of exon 2, also leading to a frame-shift and premature stop codon. Interestingly, *rKlf6<sub>bot</sub>* is very similar to *hKLF6<sub>SV1</sub>* (the shortest variant for human *KLF6*). The *hKLF6<sub>SV1</sub>* isoform has a unique 21 amino acid stretch at its C-terminus that is thought to be critical for its function; *rKlf6<sub>bot</sub>* shares 19 of these 21 amino acids.

To determine whether the shorter *rKlf6<sub>mid</sub>* and *rKlf6<sub>bot</sub>* isoforms are translated into proteins we transfected 293FT cells with V5-tagged expression constructs encoding each of the three *rKlf6* cDNA isoforms. Cells were grown in the presence or absence of proteasomal inhibitor MG132 to account for potential rapid degradation by the proteasome, since this pathway is important in the degradation of hKLF6 (13). All three rat *Klf6* isoforms were translated into protein, and were stabilized in the presence of the proteasomal inhibitor, indicating their degradation by the proteasome (Supplemental Fig. 1A). Moreover, the putative nuclear localization signal for hKLF6 lies in the C-terminus region, which is absent in *rKlf6<sub>mid</sub>* and *rKlf6<sub>bot</sub>*, indicating that the isoforms should be cytoplasmic. To verify the localization of these rat KLF6 isoforms, confocal microscopy was performed on 293FT cells transfected with V5-tagged *rKlf6* expression constructs that were immunostained for the V5 epitope tag. As predicted, rKLF<sub>top</sub> was present in both the nucleus and cytoplasm, while the two lower molecular weight isoforms, rKLF<sub>mid</sub> and rKLF<sub>bot</sub>, were unable to enter the nucleus where they displayed a cytoplasmic punctate pattern (Supplemental Fig. 1B).

By exploiting the unique splice junctions within the *rKlf6* isoforms, real-time PCR primers were designed to perform isoform-specific real time PCR (see Table 1 for list of primers). With these tools, we next assessed *rKlf6* isoform expression during stellate cell activation following liver injury, and during activation induced by primary culture on plastic (14). Rat stellate cells were isolated 24 h and 48 h after a single dose of oil (control) or CCl<sub>4</sub>. As shown in Fig. 1B, there was a dramatic decrease in levels of all *rKlf6* isoforms at 24h and 48h post injection of CCl<sub>4</sub>, and following activation in primary culture (Fig. 1C). To confirm that the cells were activating in response to culture, we assessed *collagen (I)* expression levels, which increased progressively during the culture activation as expected (Fig. 1D). To establish the relevance of these findings in rats to human stellate cells, expression of *hKLF6<sub>WT</sub>* and *hKLF6<sub>SV1</sub>* mRNAs was assessed in primary human stellate cells during culture activation. As for *rKlf6*, both human *KLF6* isoforms decreased significantly with progressive activation in culture (Fig. 1E).

### Loss of *Klf6* in hepatic stellate cells leads to more fibrogenic activity and increased liver fibrosis following liver injury

To further define the contribution of KLF6 to stellate cell activation in vivo, we next assessed the response of *Klf6* +/- mice to chronic CCl<sub>4</sub>, reasoning that loss of a single allele



of *Klf6* in stellate cells might modify their fibrogenic behavior in this model. Remarkably, there was a marked increase in inflammation along the fibrotic tracts in the *Klf6* +/- animals (Fig. 2A). Likewise, *Klf6* +/- mice displayed a marked increase in fibrotic area compared to wild type mice, as assessed by Sirius Red staining and morphometry (3.6% vs. 2.5%, p-value<0.01) with comparable levels of AST and ALT between the two groups (Fig. 2B & C). Consistent with the increased fibrosis accumulation, stellate cell-derived fibrogenic mRNAs were significantly increased in the *Klf6* +/- mice, including *Asma*, *Col1 (I)*, *Timp1*, *Timp2*,  $\beta$ -*Pdgfr*, and *Tgf- $\beta$*  mRNA transcripts, along with a decrease in levels of *Klf6* mRNA, as expected (Fig. 2D). Western blot analysis of whole liver protein lysates confirmed an increased expression of the fibrogenic proteins  $\beta$ -PDGFR, COL(I), and alpha-smooth muscle actin (ASMA) in *Klf6* +/- animals (Fig. 2E).

Because *Klf6* depletion in *Klf6* +/- mice is not restricted to stellate cells, we sought to exclude the possibility that allelic loss of *Klf6* in hepatocytes might contribute to the observed phenotype, even though the extent of injury based on serum AST and ALT levels was not affected by *Klf6* heterozygosity. To do so, we examined the impact of chronic CCl<sub>4</sub> on mice with hepatocyte-specific deletion of *Klf6* generated by crossing mice with a floxed allele of (*Klf6*<sup>F/F</sup>) (15) to animals expressing Cre-recombinase driven by the albumin promoter. In these mice, chronic CCl<sub>4</sub> did not alter fibrogenic gene expression or the extent of fibrosis as observed in the *Klf6* +/- animals (data not shown). These findings implicate loss of KLF6 in a non-parenchymal cell(s) of the liver as the reason for the observed increase in fibrosis.

To more specifically characterize the impact of KLF6 depletion on stellate cells, mouse stellate cells were isolated from *Klf6*<sup>F/F</sup> mice and activated by primary culture on plastic for 7 days. The stellate cells were then infected with adenoviruses expressing either LacZ or Cre-recombinase, and the expression of COL(I) protein was assessed by Western. As predicted, Cre-mediated deletion of *Klf6* in culture-activated stellate cells led to increased collagen expression (Fig. 2F).

### Transgenic mice with over-expression of *KLF6*<sub>WT</sub> or *KLF6*<sub>SV1</sub> in stellate cells have reduced fibrosis after injury

Despite numerous attempts to clone and characterize *Klf6* splice forms in the mouse, we repeatedly detected only one *Klf6* isoform by 5' / 3' flanking PCR. Therefore, we instead established mice expressing human isoforms as a relevant model by first establishing that the biologic activity of human splice variants in mouse stellate cells is identical to their known activity in human stellate cells. In doing so, we thereby validated the use of transgenes in which the human isoforms were expressed. In fact, the absence of multiple mouse *Klf6* isoforms facilitated our ability to attribute biology directly to human isoforms rather than through their potential interactions with mouse isoforms.

Based on our initial hypothesis that injury might be stimulating a change in the splicing pattern of KLF6, we examined the impact of over-expressing of *KLF6*<sub>WT</sub> or *KLF6*<sub>SV1</sub> on the fibrogenic activity of stellate cells. We employed the *Col1.2(I)* enhancer promoter, which is active as early as 12h after injury (16). The *KLF6*<sub>WT</sub> or *KLF6*<sub>SV1</sub> isoforms were cloned downstream of this promoter. After validating expression of the expression constructs in a mouse stellate cell line (JS1) (17) (Supplemental Fig. 2A), stellate cell specific transgenic mice were generated. At least two transgenic mouse lines were selected for efficient expression of the transgene by qRT-PCR (Supplemental Fig. 2B), and all experiments were validated in these two lines for each genotype. Because experimental findings were consistent between both mouse lines only results from a single line of *Col1.2(I)*- *KLF6*<sub>WT</sub> and *Col1.2(I)*- *KLF6*<sub>SV1</sub> mice are included.

The loss-of-function studies in *Klf6*<sup>+/-</sup> mice suggested that *Klf6* is anti-fibrotic in stellate cells, and its depletion augments their fibrogenic activity. Therefore, we next examined whether over-expression of *KLF6*<sub>WT</sub> in stellate cells would yield the opposite result, namely decreased fibrosis. Based on our characterization of the endogenous rat isoforms, as well as results from the chronic CCl<sub>4</sub> experiments in the *Klf6*<sup>+/-</sup> mice, we anticipated decreased fibrosis in the *Colα2(I)-KLF6*<sub>WT</sub> mice. As predicted, increased *KLF6*<sub>WT</sub> expression in stellate cells reduced the amount of fibrosis in mouse livers following chronic CCl<sub>4</sub> injury (Fig. 3A&C). Moreover, we anticipated the opposite phenotype in *Colα2(I)-KLF6*<sub>SV1</sub> transgenic mice, since in human cancer, *KLF6*<sub>SV1</sub> antagonizes the activity of *KLF6*<sub>WT</sub>. Surprisingly, these *Colα2(I)-KLF6*<sub>SV1</sub> mice also had dramatically decreased fibrosis, similar to *Colα2(I)-KLF6*<sub>WT</sub> transgenic mice (Fig. 3A&C). Injury levels assessed by AST and ALT were similar between the three groups (Fig. 3B). The reduced fibrosis based on morphometry was correlated with decreased expression of fibrogenic mRNAs and proteins in whole liver by real-time PCR (*Asma*, *Colα1(I)*, *Timp2*, β-*Pdgfr*, and *Tgfβ*) (Fig. 3D) and Western blot (Fig. 3E).

The reduced fibrosis in mice over-expressing *KLF6*<sub>WT</sub> or *KLF6*<sub>SV1</sub> in stellate cells could result from a decrease in total number of stellate cells following injury, a decrease in fibrogenic potential of each cell, or a combination of the two. In order to address these possibilities, we examined the fibrogenic activity of stellate cells isolated from both *Colα2(I)-KLF6*<sub>WT</sub> and *Colα2(I)-KLF6*<sub>SV1</sub> mice following acute CCl<sub>4</sub> administration. Whereas stellate cells isolated from the *Colα2(I)-KLF6*<sub>WT</sub> mice expressed significantly less *Colα1(I)*, *Colα2(I)*, and β-*Pdgfr*, fibrogenic gene expression was not altered in cells from the *Colα2(I)-KLF6*<sub>SV1</sub> animals (Fig. 4A). In order to further clarify this issue, we performed ASMA immunohistochemistry on liver sections of transgenic and wild type mice following chronic CCl<sub>4</sub> administration. Interestingly, there was a decrease in the number of ASMA positive cells in both the *Colα2(I)-KLF6*<sub>WT</sub> and *Colα2(I)-KLF6*<sub>SV1</sub> livers (Supplemental Fig. 3A & B) consistent with the possibility that the decreased fibrosis might reflect decreased numbers of activated cells in the presence of either *KLF6*<sub>WT</sub> or *KLF6*<sub>SV1</sub>.

These findings suggested that transgenic stellate cells expressing *KLF6*<sub>WT</sub> or *KLF6*<sub>SV1</sub> might be more prone to apoptosis. We therefore assessed the impact of *KLF6*<sub>WT</sub> or *KLF6*<sub>SV1</sub> on apoptosis in a human HSC line (LX2) that was stably transfected with *pBabe*, *pBabe-KLF6*<sub>WT</sub>, or *pBabe-KLF6*<sub>SV1</sub>. Indeed, apoptosis was increased in stellate cells expressing *pBabe-KLF6*<sub>WT</sub> and *pBabe-KLF6*<sub>SV1</sub> as indicated by increased PARP cleavage (Fig. 4B).

In order to confirm that *KLF6*<sub>WT</sub> was acting as a transcription factor that binds to GC boxes in the promoter regions of *Colα1(I)*, *Colα2(I)*, and β-*PDGFR*, we performed chromatin immunoprecipitation (CHIP). For this experiment, the JS1 mouse stellate cell line (JS1) was transfected with either *Colα2(I)-KLF6*<sub>WT</sub>, *Colα2(I)-KLF6*<sub>SV1</sub>, or *Colα2(I)-GFP* constructs. Based on this analysis, *KLF6*<sub>WT</sub> but not *KLF6*<sub>SV1</sub> bound to the promoters of *Colα1(I)*, *Colα2(I)*, and β-*Pdgfr* (Fig. 4C). The lack of chromatin binding by *KLF6*<sub>SV1</sub> is consistent with its lack of a DNA-binding domain. To reinforce the conclusion that *KLF6*<sub>WT</sub> can repress endogenous promoters associated with stellate cell activation, JS1 cells were transfected with *pBabe-KLF6*<sub>WT</sub> or the *pBabe* control plasmid. Similar repression was seen in the levels of *Colα1(I)*, *Colα2(I)*, and β-*Pdgfr* but not *Asma* transcripts (Fig. 4D).

## Discussion

Our data implicate *KLF6*<sub>WT</sub> as a transcription factor that preserves the quiescent phenotype of HSCs by inhibiting expression of fibrogenic genes, including *Colα1(I)*, *Colα2(I)*, and β-*Pdgfr*, as well as by inducing apoptosis of stellate cells. *KLF6*<sub>SV1</sub> normally acts as a splice

form that antagonizes KLF6<sub>WT</sub>. Interestingly, however, unlike transformed cancer cells where KLF6<sub>SV1</sub> promotes survival (6, 18), in stellate cells KLF6<sub>SV1</sub> promotes apoptosis. Moreover, because endogenous levels of KLF6 decrease with activation, there is diminishing KLF6<sub>WT</sub> for KLF6<sub>SV1</sub> to antagonize.

Our initial hypothesis that KLF6 alternative splicing yields increased antagonistic splice forms that promote stellate cell activation is refuted by this data. In fact, there are parallel decreases in full-length KLF6 (*rKlf6<sub>top</sub>*), and the shorter KLF6 isoforms (*rKlf6<sub>mid</sub>* and *rKlf6<sub>bot</sub>*) with progressive activation. The parallel decreases in expression of all isoforms suggests that the pre-mRNA for *Klf6* is reduced, resulting in similar changes for all splice isoforms, rather than due to a change in the splicing pattern.

Reduced *Klf6* mRNA levels during activation at first seem to contradict our earlier finding of transient induction during early stellate cell activation (i.e., 6–12 hours after CCl<sub>4</sub>) (1). KLF6 may have a unique role and distinct transcriptional targets early in stellate cell activation, which are different from its activities later during the activation. However, the transgenic *Colα2(I)*-promoter is only expressed at least 12 h after injury, so that the contribution of Klf6 to very early stellate cell activation cannot be assessed. Indeed, the findings suggest that Klf6 may be solely anti-fibrogenic. The early, transient peak of *Klf6* mRNA immediately following injury could serve to preserve cellular quiescence in order to prevent unwanted, premature activation of stellate cells. Thereafter, decreasing expression of *Klf6* mRNA could enable cells to activate. This role of KLF6 as a potential 'quiescence-preserving' gene is consistent with findings for another transcription factor, Lhx2, whose absence in development leads to spontaneous neonatal liver fibrosis (19).

The findings of reduced fibrosis in *Klf6*<sup>+/-</sup> mice suggest that allelic loss of *Klf6* in stellate cells might contribute to increased fibrosis. However, because heterozygosity is present in all cell types, the observed phenotype cannot be definitively ascribed directly to KLF6 loss in stellate cells. Moreover, *Klf6*<sup>+/-</sup> mice displayed an increased inflammatory infiltrate in liver after CCl<sub>4</sub>, compared to wild type animals, raising the prospect that loss of KLF6 in the inflammatory cells might alter their response to injury even though AST and ALT levels after CCl<sub>4</sub> were unaffected by *Klf6* heterozygosity. A more specific way to establish that stellate cell specific loss of KLF6 leads to increased fibrosis would be to cross *Klf6*<sup>F/F</sup> mice with GFAP-Cre mice. However, this attempt resulted in a profound neurologic phenotype in mice, which precluded analysis of liver injury (data not shown). Studies using isolated stellate cells from *Klf6*<sup>F/F</sup> mice support the idea that loss of KLF6 in stellate cells is an important contributor to enhanced fibrosis.

Data from mice with transgenic expression of *KLF6*<sub>WT</sub> or *KLF6*<sub>SV1</sub> is complementary and supports an antifibrotic role of this gene. Reduced fibrosis in mice over-expressing KLF6<sub>WT</sub> or KLF6<sub>SV1</sub> in stellate cells reflects either a decrease in stellate cell numbers following injury, a decrease in fibrogenic potential of each cell, or the combination of the two. The experiments utilizing stable over-expression of KLF6<sub>WT</sub> or KLF6<sub>SV1</sub> in hepatic stellate cells demonstrate an increase in apoptosis in both cases. Furthermore, although stellate cells isolated from the *Colα2(I)-KLF6*<sub>WT</sub> mice expressed significantly less *Colα1(I)*, *Colα2(I)*, and  $\beta$ -*Pdgfr*, fibrogenic gene expression was not altered in cells from the *Colα2(I)-KLF6*<sub>SV1</sub> animals. KLF6<sub>WT</sub> but not KLF6<sub>SV1</sub> interacts directly with 'GC' boxes in the promoter regions of *Colα1(I)*, *Colα2(I)*, and  $\beta$ -*Pdgfr*. These data, combined with findings following the over-expression of KLF6<sub>WT</sub> in JS1 cells demonstrating transcriptional inhibition, suggest that KLF6<sub>WT</sub> directly represses these promoters. In short, the phenotype in the *KLF6*<sub>WT</sub> transgenic mice is due to both a decrease in fibrogenic potential, as well as decreasing stellate cell number, which is likely as a result of increased apoptosis.



KLF6 is a well studied transcription factor that can repress or activate target genes by interacting with co-regulator proteins such as HDACs (20). A recent paper implicates ligand-dependent corepressor (LCoR), in the regulation of KLF6 target genes (21), notably p21, and E-cadherin. Promoter bound KLF6 inhibits downstream genes by tethering a transcriptional co-repressor complex containing LCoR, with specific contributions by C-terminal binding protein (CtBP1), and HDACs. It would be informative to determine which co-regulator proteins interact with KLF6 during the inhibition of fibrogenic genes in quiescent stellate cells.

In summary, our findings clarify the role of KLF6 and its isoforms during hepatic stellate cell activation. Moreover, the parallel activities of both KLF6<sub>WT</sub> and its splice isoforms contrasts entirely with their behavior in human cancer (6, 7, 12, 18), reinforcing the conclusion that activities of splice isoforms may be highly context-dependent not only for KLF6, but possibly other genes that are alternatively spliced.

## Supplementary Material

Refer to Web version on PubMed Central for supplementary material.

## Acknowledgments

**Grant support:** MSTP Grant to ZGN, DK56621, DK47340 and P20AA017067 to SLF, Summer Student support from MSSM

## Abbreviations

<b>KLF6</b>	Kruppel like factor 6
<b>KLF6<sub>WT</sub></b>	KLF6 wild type
<b>KLF6<sub>SV1</sub></b>	KLF6 splice variant 1
<b>HSC</b>	Hepatic stellate cell

## REFERENCES

1. Ratziu V, Lalazar A, Wong L, Dang Q, Collins C, Shaulian E, Jensen S, et al. Zf9, a Kruppel-like transcription factor up-regulated in vivo during early hepatic fibrosis. *Proc Natl Acad Sci U S A*. 1998; 95:9500–9505. [PubMed: 9689109]
2. Botella LM, Sanchez-Elsner T, Sanz-Rodriguez F, Kojima S, Shimada J, Guerrero-Esteo M, Cooreman MP, et al. Transcriptional activation of endoglin and transforming growth factor-beta signaling components by cooperative interaction between Sp1 and KLF6: their potential role in the response to vascular injury. *Blood*. 2002; 100:4001–4010. [PubMed: 12433697]
3. Kremer-Tal S, Narla G, Chen Y, Hod E, Difeo A, Yea S, Lee JS, et al. Downregulation of KLF6 is an early event in hepatocarcinogenesis, and stimulates proliferation while reducing differentiation. *J Hepatol*. 2007; 46:645–654. [PubMed: 17196295]
4. Narla G, Heath KE, Reeves HL, Li D, Giono LE, Kimmelman AC, Glucksman MJ, et al. KLF6, a candidate tumor suppressor gene mutated in prostate cancer. *Science*. 2001; 294:2563–2566. [PubMed: 11752579]
5. Kremer-Tal S, Reeves HL, Narla G, Thung SN, Schwartz M, Difeo A, Katz A, et al. Frequent inactivation of the tumor suppressor Kruppel-like factor 6 (KLF6) in hepatocellular carcinoma. *Hepatology*. 2004; 40:1047–1052. [PubMed: 15486921]
6. Narla G, DiFeo A, Fernandez Y, Dhanasekaran S, Huang F, Sangodkar J, Hod E, et al. KLF6-SV1 overexpression accelerates human and mouse prostate cancer progression and metastasis. *J Clin Invest*. 2008; 118:2711–2721. [PubMed: 18596922]

7. DiFeo A, Narla G, Hirshfeld J, Camacho-Vanegas O, Narla J, Rose SL, Kalir T, et al. Roles of KLF6 and KLF6-SV1 in ovarian cancer progression and intraperitoneal dissemination. *Clin Cancer Res.* 2006; 12:3730–3739. [PubMed: 16778100]
8. Matsumoto N, Kubo A, Liu H, Akita K, Laub F, Ramirez F, Keller G, et al. Developmental regulation of yolk sac hematopoiesis by Kruppel-like factor 6. *Blood.* 2006; 107:1357–1365. [PubMed: 16234353]
9. Blomhoff R, Berg T. Isolation and cultivation of rat liver stellate cells. *Methods Enzymol.* 1990; 190:58–71. [PubMed: 1965004]
10. Lalazar A, Wong L, Yamasaki G, Friedman SL. Early genes induced in hepatic stellate cells during wound healing. *Gene.* 1997; 195:235–243. [PubMed: 9305769]
11. Narla G, Difeo A, Reeves HL, Schaid DJ, Hirshfeld J, Hod E, Katz A, et al. A germline DNA polymorphism enhances alternative splicing of the KLF6 tumor suppressor gene and is associated with increased prostate cancer risk. *Cancer Res.* 2005; 65:1213–1222. [PubMed: 15735005]
12. Narla G, DiFeo A, Yao S, Banno A, Hod E, Reeves HL, Qiao RF, et al. Targeted inhibition of the KLF6 splice variant, KLF6 SV1, suppresses prostate cancer cell growth and spread. *Cancer Res.* 2005; 65:5761–5768. [PubMed: 15994951]
13. Banck MS, Beaven SW, Narla G, Walsh MJ, Friedman SL, Beutler AS. KLF6 degradation after apoptotic DNA damage. *FEBS Lett.* 2006; 580:6981–6986. [PubMed: 17113081]
14. De Minicis S, Seki E, Uchinami H, Kluwe J, Zhang Y, Brenner DA, Schwabe RF. Gene expression profiles during hepatic stellate cell activation in culture and in vivo. *Gastroenterology.* 2007; 132:1937–1946. [PubMed: 17484886]
15. Leow CC, Wang BE, Ross J, Chan SM, Zha J, Carano RA, Frantz G, et al. Prostate-specific Klf6 inactivation impairs anterior prostate branching morphogenesis through increased activation of the Shh pathway. *J Biol Chem.* 2009; 284:21057–21065. [PubMed: 19494112]
16. Inagaki Y, Truter S, Bou-Gharios G, Garrett LA, de Crombrughe B, Nemoto T, Greenwel P. Activation of Proalpha2(I) collagen promoter during hepatic fibrogenesis in transgenic mice. *Biochem Biophys Res Commun.* 1998; 250:606–611. [PubMed: 9784393]
17. Guo J, Loke J, Zheng F, Hong F, Yea S, Fukata M, Tarocchi M, et al. Functional linkage of cirrhosis-predictive single nucleotide polymorphisms of Toll-like receptor 4 to hepatic stellate cell responses. *Hepatology.* 2009; 49:960–968. [PubMed: 19085953]
18. DiFeo A, Feld L, Rodriguez E, Wang C, Beer DG, Martignetti JA, Narla G. A functional role for KLF6-SV1 in lung adenocarcinoma prognosis and chemotherapy response. *Cancer Res.* 2008; 68:965–970. [PubMed: 18250346]
19. Wandzioch E, Kolterud A, Jacobsson M, Friedman SL, Carlsson L. Lhx2<sup>-/-</sup> mice develop liver fibrosis. *Proc Natl Acad Sci U S A.* 2004; 101:16549–16554. [PubMed: 15536133]
20. Li D, Yea S, Li S, Chen Z, Narla G, Banck M, Laborda J, et al. Kruppel-like factor-6 promotes preadipocyte differentiation through histone deacetylase 3-dependent repression of DLK1. *J Biol Chem.* 2005; 280:26941–26952. [PubMed: 15917248]
21. Calderon MR, Verway M, An BS, DiFeo A, Bismar TA, Ann DK, Martignetti JA, et al. Ligand-dependent corepressor (LCoR) recruitment by Kruppel-like factor 6 (KLF6) regulates expression of the cyclin-dependent kinase inhibitor CDKN1A gene. *J Biol Chem.* 287:8662–8674. [PubMed: 22277651]

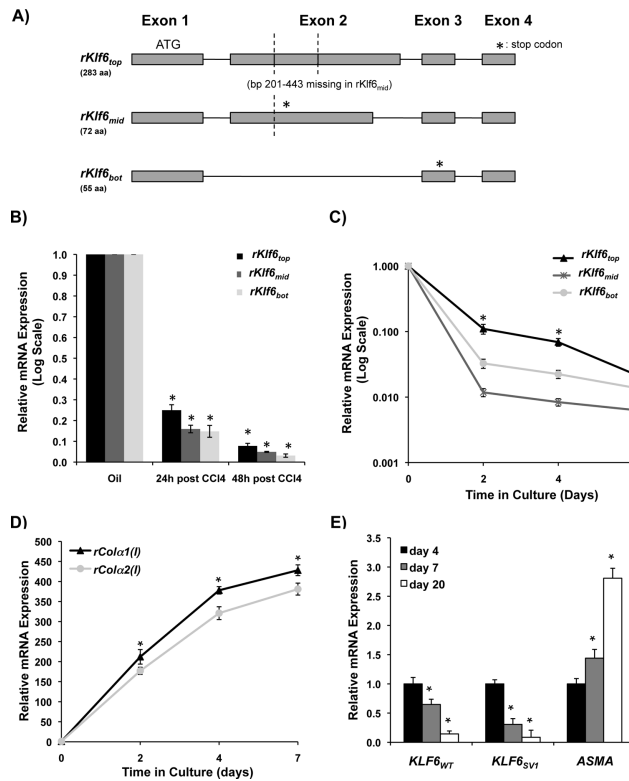


**Figure 1. KLF6 isoforms in human and rat stellate cells decrease with activation of these cells**  
**A.** Primary rat HSC cDNA from a normal rat was used as template in PCR reaction with primers designed to the 5' and 3' UTRs of rat *Klf6* transcript. Three DNA products were present, which were cloned, sequenced and aligned with rat genome, confirming 3 *Klf6* splice isoforms shown; **B.** Rats were injected once with either oil, or CCl<sub>4</sub> followed by HSC isolation 24h and 48h thereafter (n=3 for each treatment and time point). Rat *Klf6* isoform levels were assessed by qRT-PCR with isoform-specific primers, demonstrating a significant decrease for all 3 isoforms (p-value<0.001) (data was normalized to GAPDH, fold change was calculated by comparing CCl<sub>4</sub> and oil samples); **C.** Primary rat stellate cells (3 separate isolates) from untreated rats were plated in primary culture for 7 days, and all *Klf6* isoforms decreased similar to stellate cells analyzed following liver injury in vivo (p-value<0.01) (data was normalized to GAPDH, fold change was calculated by comparing days 2, 4, and 7 to day 0); **D.** *Collagen (I)* mRNA increases during primary culture confirming that cells responded as expected to culture-induced activation; **E.** Human *KLF6* isoforms (*KLF6<sub>WT</sub>* and *KLF6<sub>SVI</sub>*) are both down-regulated following primary culture of human stellate cells isolated from normal liver (3 separate isolations, p-value<0.05).

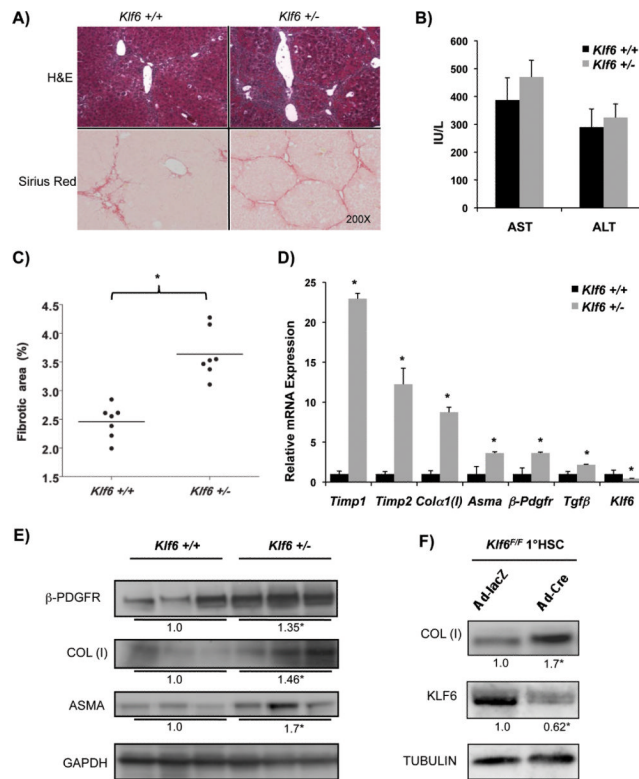


**Figure 2. KLF6 deficiency in *Klf6*<sup>+/-</sup> mice leads to increased fibrogenesis following CCl<sub>4</sub> liver injury with similar results obtained using knockdown of Klf6 in cultured *Klf6*<sup>F/F</sup> stellate cells A&C.** Increased fibrosis *Klf6*<sup>+/-</sup> mice following 8 weeks of chronic CCl<sub>4</sub>, compared to *Klf6*<sup>+/+</sup> mice (n=7/group) (3.6% vs. 2.5%, p-value<0.01)(For each animal, 40 images were taken at low magnification (10X objective lens), and were subsequently used for quantifying percentage of fibrotic tissue using BioQuant Software) **B.** Both groups showed comparable liver injury levels as demonstrated by equally elevated AST and ALT; **D.** Whole liver sample qRT-PCR from the same mice, shows an increase in HSC-derived fibrogenic mRNA in *Klf6* deficient livers (p-value<0.01); **E.** Whole liver protein Western blot of 3 representative samples from *Klf6*<sup>+/-</sup> and *Klf6*<sup>+/+</sup> mice after chronic CCl<sub>4</sub> documenting increased fibrogenic proteins COL (I), *β*-PDGFR, and ASMA; **F.** *Klf6*<sup>F/F</sup> stellate cells were isolated from mice and allowed to activate for 1 week in culture, followed by infection with Ad-lacZ or Ad-Cre (MOI=10) and analyzed 48h later. Cells with a *Klf6* knockdown show an increase in COL (I).

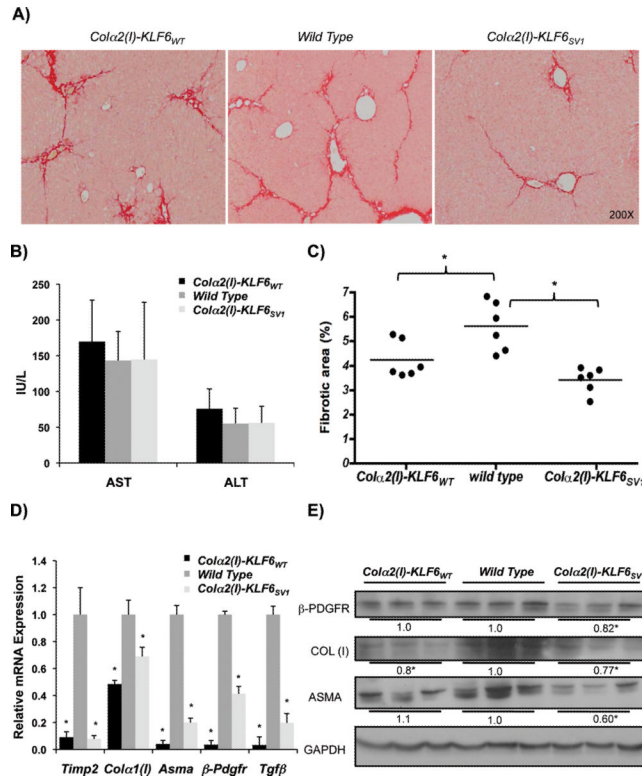


**Figure 3. Stellate cell specific *KLF6<sub>WT</sub>* and *KLF6<sub>SV1</sub>* transgenic mice have decreased fibrosis following CCl<sub>4</sub> liver injury**

**A&C.** Decreased fibrosis based on Sirius Red morphometry in *Colα2(I)-KLF6<sub>WT</sub>* and *Colα2(I)-KLF6<sub>SV1</sub>* mice following 8 weeks of chronic CCl<sub>4</sub> compared to wild type littermates (n=6/group) (4.2% and 3.4% respectively compared to 5.6%, p-value<0.01)(For each animal, 40 images were taken at low magnification (10X objective lens), and were subsequently used for quantifying percentage of fibrotic tissue using BioQuant Software); **B.** Levels of AST and ALT were comparable between WT and transgenic mice after chronic CCl<sub>4</sub> injury; **D.** Decreased HSC-derived fibrogenic mRNAs in whole liver from *Colα2(I)-KLF6<sub>WT</sub>* and *Colα2(I)-KLF6<sub>SV1</sub>* mice compared to wild type littermates (p-value<0.01); **E.** Parallel decrease in fibrogenic proteins COL (I), β-PDGFR, and ASMA for *Colα2(I)-KLF6<sub>SV1</sub>* mice and a decrease in COL (I) for *Colα2(I)-KLF6<sub>WT</sub>* mice based on western blot of whole liver lysates from 3 representative mice/group after chronic CCl<sub>4</sub>.



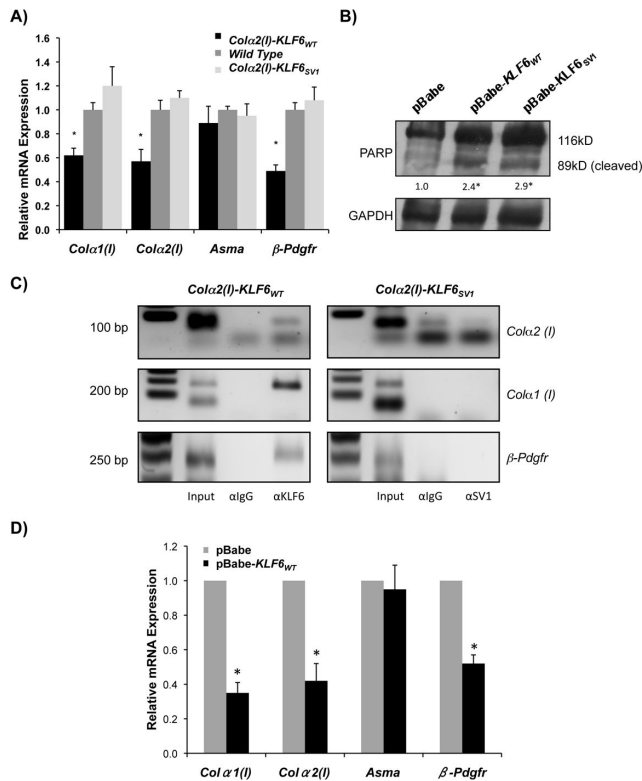


**Figure 4. KLF6<sub>WT</sub> transcriptionally inhibits *Colα1(I)*, *Colα2(I)*, and  $\beta$ -*Pdgfr*; both KLF6 isoforms lead to increased apoptosis of stellate cells in vitro**

**A.** Mouse stellate cells were isolated from *Colα2(I)-KLF6<sub>WT</sub>*, *Colα2(I)-KLF6<sub>SV1</sub>*, and wild type mice (5 mice each) following 3 doses of CCl<sub>4</sub>. A decrease in fibrogenic gene expression in *Colα2(I)-KLF6<sub>WT</sub>*, but not *Colα2(I)-KLF6<sub>SV1</sub>* transgenic stellate cells is evident in fresh HSC isolates; **B.** Increased apoptosis in human stellate cell lines (LX2) following stable transfection of pBabe-KLF6<sub>WT</sub>, or pBabe-KLF6<sub>SV1</sub>, based on the presence of cleaved form of PARP; **C.** Immortalized mouse stellate cells (JS1) transfected with *Colα2(I)-KLF6<sub>WT</sub>*, or *Colα2(I)-KLF6<sub>SV1</sub>* constructs, and samples were prepared for chromatin IP 48h after transfection. Primer sets specific for GC boxes in promoter regions (2kb region upstream of start site) of *Colα1(I)*, *Colα2(I)*, and  $\beta$ -*Pdgfr* demonstrate binding of KLF6<sub>WT</sub>, but not KLF6<sub>SV1</sub> to all three promoters; **D.** mouse stellate cells (JS1) over-expressing pBabe-KLF6<sub>WT</sub> show decreased transcript levels of *Colα1(I)*, *Colα2(I)*, and  $\beta$ -*Pdgfr* (p-value<0.05).

Table 1

## List of Primers

Name	Sequence
rKlf6 Bot F	5'-ACTCCTGATCGTTCACCTCCCTG-3'
rKlf6 Bot R	5'-GTAAGGCTTTTCTCCTGTTGCCAAT-3'
rKlf6 Mid F	5'-CGAAACGGGCTACTTCTCGGCT-3'
rKlf6 Mid R	5'-TTCGGGAGAAGAAGGATTTTGGT-3'
rKlf6 Top F	5'-CGGGAGAGGAAGGAGGAATCAGA-3'
rKlf6 Top R	5'-AGAGGTAAACTTGGTTCGTGGGC-3'
rGAPDH F	5'-GGCATCGTGGAAGGGCTCAT-3'
rGAPDH R	5'-AGGGATGATGTTCTGGGCTGC-3'
rCOLa2 (I) F	5'-TGAGCCTGGTGAGCCCG-3'
rCOLa2 (I) R	5'-TCTCGCCAGGTCTTCCAGG-3'
rCola1 (I) F	5'-GTGTAACGATGGTGTCTGTC-3'
rCola1 (I) R	5'-CTTACCCTTAGCACCAGC-3'
rASMA F	5'-GCTGTCTTCCCATCCATCGTG-3'
rASMA R	5'-TGGGGTACTTCAGATCAGGATG-3'
rPDGFBR F	5'-CATTGGGGACAGGAAGTGGAC-3'
rPDGFBR R	5'-CCTGATGGTGATGCTCTCGC-3'
rTGFB1 F	5'-CACAAACAGTGGCAGCGGGAC-3'
rTGFB1 R	5'-CAGAGGTGGCAGAAACTGTAATG-3'
rMMP2 F	5'-GACGGCAAATATGGCTTCTGTCC-3'
rMMP2 R	5'-GCCCTCGGTGGTACAGC-3'
rTIMP1 F	5'-GCCTACACCCAGCCAT-3'
rTIMP1 R	5'-ATGCCAGGAACCAAGGAGC-3'
rTIMP2 F	5'-GGCAACCCATCAAGAGGATTCAAT-3'
rTIMP2 R	5'-CACACTGCTGAGGAGGGG-3'
mGAPDH F	5'-CAATGACCTTCATTGACC-3'
mGAPDH R	5'-GATCTCGCTCCTGGAAGATG-3'
mCOLa1 (I) F	5'-GTCCCTGAAGTCAGCTGCATA-3'
mCOLa1 (I) R	5'-TGGGACAGTCCAGTTCTTCAT-3'
mASMA F	5'-TCCTCCCTGGAGAAGAGCTAC-3'
mASMA R	5'-TATGGTGGTTTCGTGGATGC-3'
mTGFB F	5'-TGCGCTTGCAGAGATTAATA-3'
mTGFB R	5'-CTGCCGTACAACCTCCAGTGA-3'
mMMP2 F	5'-ACCCAGATGTGGCCAACTAC-3'
mMMP2 R	5'-TACTTTTAAGGCCGAGCAA-3'
mTIMP2 F	5'-GCCAAAGCAGTGAGCGAGAAG-3'
mTIMP2 R	5'-CACACTGCTGAAGAGGGGGC-3'
mTIMP1 F	5'-ACGAGACCACCTTATACCAGCG-3'
mTIMP1 R	5'-GCGGTCTGGGACTTGTGGGC-3'
mCOLa2 (I) F	5'-GTGTTCTGGTCTCAGGGT-3'

<b>Name</b>	<b>Sequence</b>
mCOLa2 (I) F	5'-GTCTGAGTGAAGGCTGGGAG -3'
mTGFbR1 F	5'-ACTGAAAGCTTCCCAGGGTT-3'
mTGFbR1 R	5'-TAAGGGCTGGCAGTTGTCTT-3'
mPDGFRB F	5'-CTTTGTGCCAGATCCCACCA-3'
mPDGFRB R	5'-TCACTCGGCACGGAATTGTC-3'